

This is the author's peer reviewed, accepted manuscript. However, the online version of record will be different from this version once it has been copyedited and typeset.

PLEASE CITE THIS ARTICLE AS DOI: 10.1063/1.50003590

Oxide 2D Electron Gases as a Reservoir of Defects for Resistive Switching

Dror Miron,¹ Dana Cohen Azarzar¹, Barak Hoffer¹, Maria Baskin¹,
Shahar Kvatinsky¹, Eilam Yalon¹ and Lior Kornblum^{1,a)}

¹The Andrew & Erna Viterbi Department of Electrical Engineering, Technion - Israel Institute of Technology, Haifa 32000, Israel

A non-volatile resistive switching device is demonstrated, utilizing a 2D electron gas (2DEG) between a SrTiO₃ (STO) substrate and an amorphous Al₂O₃ layer. A large resistance window is observed and its origin discussed. We pinpoint the role of the oxide interface in enabling the resistive switching behavior. The switching mechanism is proposed to be filamentary type that is formed inside the Al₂O₃ layer, the result of oxygen vacancies that are driven from the interface into the insulating Al₂O₃ under high electric fields. These results highlight the concept of memristive devices where the 2DEG serves both as the back electrode and as the source of defects necessary for resistive switching, providing a simple and scalable process for future devices.

^{a)} Author to whom correspondence should be addressed. Electronic mail: liork@ee.technion.ac.il

This is the author's peer reviewed, accepted manuscript. However, the online version of record will be different from this version once it has been copyedited and typeset.

PLEASE CITE THIS ARTICLE AS DOI: 10.1063/1.50003590

The formation of a conductive interface between two insulating oxides, often the result of a two dimensional electron gas¹ (2DEG), heralded massive interest into its fundamental physics²⁻⁵, and more recently in devices that leverage this phenomenon⁶. Examples include field-effect transistors with 2DEG channels⁷, chemical sensors^{8,9}, and optoelectronic devices^{10,11}. A few resistive switching demonstrations have been reported with conductive oxide interfaces: Wu et al. explored resistive switching devices¹² where oxygen vacancies inside LaAlO₃ are a possible source of filamentary conduction. Kim et al. have recently reported an ionic conductive bridge resistive switching device where metal ions from the top electrode form the conductive bridge¹³; in both these demonstrations the conductive oxide interface served as the back electrode.

While other interesting candidates have recently emerged, SrTiO₃ (STO) is by far the most studied substrate for forming conductive oxide interfaces⁴. Oxygen vacancies in STO provide a rich spectrum of electronic properties¹⁴⁻¹⁷, allowing thermodynamic and kinetic control over the material's electrical behavior¹⁸⁻²¹. As such, STO has been of significant interest as a memristive material^{22,23}.

Most devices based on conductive oxide interfaces demonstrated to date were based on pulsed laser deposition (PLD) growth of epitaxial LaAlO₃ layers on SrTiO₃ substrates. Nonetheless, Chen et al. demonstrated conductivity at non-epitaxial interfaces²⁴, where the conductivity has been ascribed to oxygen vacancies near the interface. Particular recent attention has been focused on non-epitaxial conductive interfaces fabricated by the scalable and microelectronics-compatible atomic layer deposition (ALD) process, which promises considerable practical advantages over epitaxial interfaces^{13,25-28}.

This is the author's peer reviewed, accepted manuscript. However, the online version of record will be different from this version once it has been copyedited and typeset.

PLEASE CITE THIS ARTICLE AS DOI: 10.1063/1.50003590

In this work, we leverage the conductivity formed at the non-epitaxial interface between ALD- Al_2O_3 and SrTiO_3 for resistive switching devices. We obtain a large memory window and suggest that it is the consequence of the highly insulating Al_2O_3 layer. We propose a mechanism in which the conductive interface functions both as a conductive back electrode, and as a reservoir of oxygen defects that form the filamentary switching, thus enabling to preserve the high resistivity of the insulator in the off state.

Ion bombardment,²⁹ UV radiation,³⁰ deposition damage³¹ and chemical reduction³² are some of the known routes for creating conductive STO surfaces, where the degree of 2D confinement might be low. Within the current context, we do not discuss the degree of interfacial confinement of the electrons and use of the term 2DEGs loosely; we acknowledge that the interface conductivity may extend nanometers inside the STO. We will show that the interface serves as a useful back electrode, and as a source of defects for filamentary switching of the Al_2O_3 ; both these roles are unrelated to the exact 2D nature of the electrons.

(001) TiO_2 -terminated undoped $5\times 5\text{ mm}^2$ STO crystals (CrysTec GmbH) served as the substrate. Nominally 10 nm thick amorphous Al_2O_3 layer was grown by atomic layer deposition (ALD, Ultratech/Cambridge Nanotech Fiji G2) using trimethyl-aluminum (TMA) and water as the precursors. The full ALD details are specified in our previous work³³ (where they were referred to as 'Recipe B'), with an addition of a pre-treatment for surface activation (NH_3 plasma for 120 s immediately followed by Al_2O_3 deposition). An earlier report on similar Al_2O_3 has confirmed its amorphous structure (supplement of Ref. ³⁴). Van der Pauw measurements at room temperature yield a sheet resistance of $\sim 400\ \Omega/\text{sq}$, confirming the suitability of the interface as a back electrode of the device. This value

This is the author's peer reviewed, accepted manuscript. However, the online version of record will be different from this version once it has been copyedited and typeset.

PLEASE CITE THIS ARTICLE AS DOI: 10.1063/1.50003590

is lower than typical values for LAO/STO¹⁷ and it is likely that the conductivity is not confined to the interface extends into the STO.

Contacts to the conductive interface were formed by scribing regions at the edge of the sample and depositing 200 nm of Al (Figure 1a). Top electrodes were formed by 50 nm Pt pads (of areas between $2.7 \times 10^{-4} \text{ cm}^2$ to $1.5 \times 10^{-3} \text{ cm}^2$) deposited through a shadow mask, where both metallizations were done using e-beam evaporation.

The electrical behavior of the devices was analyzed using current voltage (IV) measurements using a Keithely 2450 source meter SMU instrument.

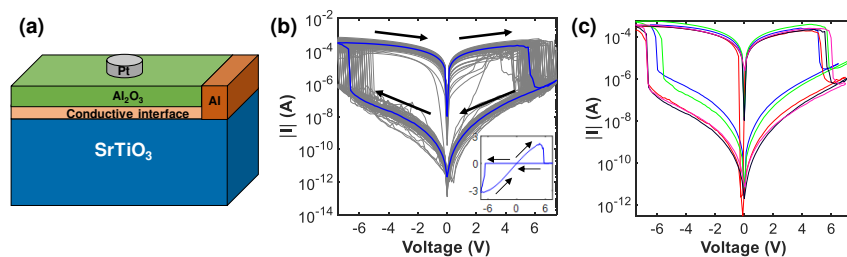


Figure 1. (a) Schematic view of Pt/Al₂O₃/STO structures, (b) 100 IV switching cycles (median is highlighted in blue). Inset shows an IV plot of the median curve on a linear scale (same axes and units). The arrows indicate the sweeping direction. (c) Median IV plots of 5 different devices.

Forming of the Pt/Al₂O₃/STO structure was detectable in the range of -6 to -4 V at a current compliance of 0.1 mA. After forming the structures were evaluated by 100 IV sweeps. Each plot is composed of a forward voltage sweep from -7.5 V to 7.5 V, and a backward voltage sweep from 7.5 V to -7.5 V. The IV results (Figure 1b) exhibit robust and abrupt switching both for set and reset events. From these 100 cycles, a median curve was determined, and cycle-to-cycle variability is observed, to be addressed later on. It is noted that there are wide memory window regions unaffected by the variability (-4 to -1 V

This is the author's peer reviewed, accepted manuscript. However, the online version of record will be different from this version once it has been copyedited and typeset.

PLEASE CITE THIS ARTICLE AS DOI: 10.1063/1.50003590

and +1 to +3 V, Figure 1b). Identical analysis was performed on 4 additional devices on the same sample, showing variability that is smaller than the cycle-to-cycle variability.

The set and reset voltages are plotted as a histogram in Figure 2a, showing the number of cycles (counts) at which every set/reset voltage was extracted, at a resolution of 0.5 V. The set voltages range from -5 V to -7.5 V, and the reset voltages range from 4.3 V to 7 V.

Two distinguished resistive states, a high resistive state (HRS) and a low resistive state (LRS), were labelled according to their resistances as R_{HRS} and R_{LRS} . These resistances were determined by dividing the read voltage at 0.1 V by the corresponding current and are presented as a histogram of cumulative probabilities in Figure 2b. It can be observed from this histogram that in 90% of the cycles, R_{LRS} was below 100 k Ω , while R_{HRS} was over 3.5 G Ω in all cycles, indicative of a large separation between states of above 4 orders of magnitude.

To better understand the DC endurance behavior of this sample, the HRS and LRS resistances were plotted as a function of the cycle number (Figure 2c). Within these 100 cycles it is noticeable that there are a few cycles (5%) in which switching did not occur (R_{LRS} in the R_{HRS} region). It is noted that using the slow DC sweeps as a gauge of endurance forces much harsher conditions than practical working conditions of the memristive device (*i.e.* pulses). However, to thoroughly understand and compare the endurance of the device to the technology requirements, application a train of pulsed voltage stress is necessary³⁵.

This is the author's peer reviewed, accepted manuscript. However, the online version of record will be different from this version once it has been copyedited and typeset.

PLEASE CITE THIS ARTICLE AS DOI: 10.1063/1.50003590

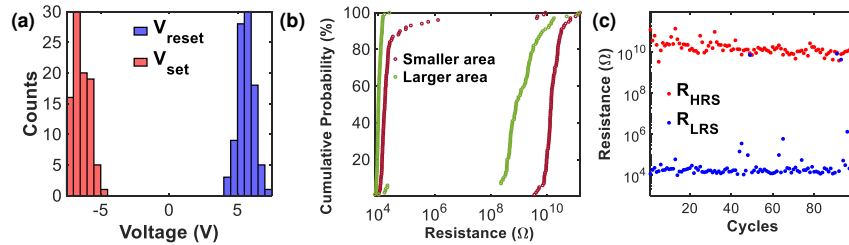


Figure 2. Analysis of the switching statistics of a Pt/Al₂O₃/STO device based on 100 DC IV sweeps. (a) Histogram of set and reset voltages. (b) Histogram of cumulative probabilities of R_{HRS} and R_{LRS}, measured for two Pt pad areas. (c) Endurance plot for 100 cycles of DC IV sweeps.

We suggest that the observed switching behavior originates from conductive filaments that form inside the Al₂O₃ layer and allow the ohmic properties that characterize the samples in the LRS (inset of Figure 1b). Different pads of sizes between $1.5 \times 10^{-3} \text{ cm}^2$ to $2.7 \times 10^{-4} \text{ cm}^2$ did not yield any dependence of the measured resistance on the pads' area, which further implies a filamentary resistive switching^{22,36}.

When considering the question of the physical origin of the observed filamentary behavior we face 2 possible sources: the Al₂O₃ layer, which can sometimes show resistive switching^{37,38} or the Al₂O₃/STO interface.

We previously studied a similar ALD-Al₂O₃ layer, grown by the same recipe on Nb:STO (minus the surface activation step)³³. The electrical behavior of the Al₂O₃ layer grown on the different substrates is compared in Figure 3. Nearly identical current-density voltage (JV) curves in the pre-forming state (Figure 3) support the assumption regarding the similarity of the Al₂O₃ layers. Since we observed no hysteresis or resistive switching behavior when measuring the device grown on Nb:STO, we conclude that the filamentary behavior observed in the current work does not originate from the Al₂O₃ layer. This conclusion highlights the conductive interface as the source of the resistive switching

This is the author's peer reviewed, accepted manuscript. However, the online version of record will be different from this version once it has been copyedited and typeset.

PLEASE CITE THIS ARTICLE AS DOI: 10.1063/1.50003590

behavior in the current device. We further point out that our previous study of similar Al_2O_3 layers³⁴ with x-ray photoelectron (XPS) analysis of the Al 2p region have shown only the +3 state, implying that the initial vacancy concentration is well below the $\sim 2\%$ detection limit of this analysis.

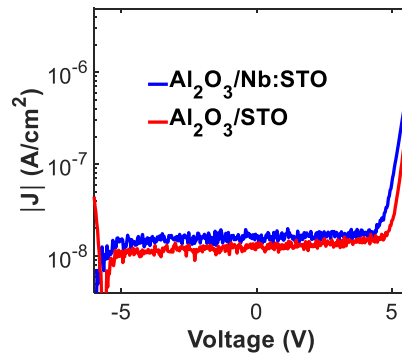


Figure 3. Comparison of the leakage current between the same Al_2O_3 recipe used to grow on Nb:STO³³ and on undoped STO with a conductive interface used in this work.

Therefore, we ascribe this resistive switching behavior to a filament type mechanism based on drift of oxygen vacancies³⁹. The interfacial conductivity at the Al_2O_3 -STO interface is attributed to oxygen vacancies^{25,40}, which is further acting as a reservoir for oxygen vacancies; under large negative gate bias these positively-charged defects are attracted towards the metal electrode and thus drift into the Al_2O_3 ; by this the vacancies form a conductive filament (Figure 4a), which switches the device on into its LRS state. The opposite occurs at a large enough positive bias, under which some of the oxygen vacancies drift back towards substrate, making the filaments shorter and thus breaking the conductive path, switching the device off into its HRS state (Figure 4b). Using a vacancy-rich layer as a reservoir for defects to be injected into a higher-resistance layer is a well-

This is the author's peer reviewed, accepted manuscript. However, the online version of record will be different from this version once it has been copyedited and typeset.

PLEASE CITE THIS ARTICLE AS DOI: 10.1063/1.50003590

known strategy in other materials^{41–43}; however the current work utilizes the substrate for this purpose, as well as for the back electrode, which circumvents an additional layer.

Other mechanisms which are associated with resistive switching were previously reported; these include charge trapping and detrapping⁴⁴, polaron melting and ordering⁴⁵, electric field induced generation of crystalline defects^{46,47} and electrochemical migration⁴⁸. However, in case that one of the abovementioned mechanisms is the dominant resistive switching mechanism, then we would expect to observe the switching to also occur in the structure without the conducting interface. Lack of such an observation³³ leads to the conclusion that oxygen vacancies have the most significant role in the switching process, as indicated by others^{49–51}. Another possible mechanism for switching might be field-induced rearrangement of the vacancies at the $\text{Al}_2\text{O}_3/\text{STO}$ interface, which might affect the interface barrier height^{52,53}. However, since switching is clearly observed in both negative and positive voltages (Fig. 1b), changes of just one of the barriers cannot account for this behavior, further pointing towards the role of the Al_2O_3 layer itself in switching.

Oxygen vacancies in Al_2O_3 were shown to form defects in the band gap at an estimated energy level of 2 eV beneath the conduction band^{54–56}, which can promote leakage currents³³. One could further consider the role of the Pt electrode in the resistive switching, in light of reports that bias might affect the bonding at Pt- HfO_2 interfaces.⁵⁷ However, we note that for the present case no hysteresis was observed in neither capacitance-voltage⁵⁸ nor current-voltage³³ analysis of Pt- Al_2O_3 , with the latter being essentially the same sample structure minus the conducting interface. This further validates the interface role as the origin of the resistive switching behavior, by serving as a defects reservoir.

This is the author's peer reviewed, accepted manuscript. However, the online version of record will be different from this version once it has been copyedited and typeset.

PLEASE CITE THIS ARTICLE AS DOI: 10.1063/1.50003590

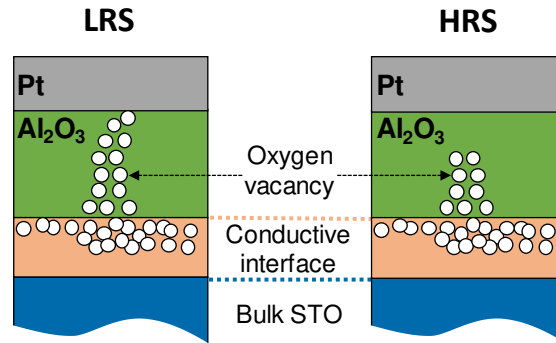


Figure 4. Schematic illustrations showing the proposed switching based on oxygen vacancies. (a) LRS, and (b) HRS.

A Pt/Al₂O₃/STO non-volatile resistive switching device was demonstrated, showing a large resistance window. This large window is attributed to the highly insulating Al₂O₃ layer, as manifested by the high resistance values in the HRS (> 3.5 GΩ). The large switching voltages observed here (< 7.5 V) could be reduced by the application of thinner insulator layer, where lower voltages are needed to obtain the same electric field that drives the vacancies.⁵⁹ The large resistance window leaves ample room for thinning the insulator while maintaining sufficiently large window.

Analysis of the switching mechanism points to a filamentary type. This filament is composed out of oxygen vacancies that are available from the conductive interface. While similar conductive interfaces have been employed for various applications, we propose utilizing this interface both the back electrode and the source of oxygen vacancies. These observations can promote future concepts of memristive devices, using the scalable ALD process.

Supplementary Material

This is the author's peer reviewed, accepted manuscript. However, the online version of record will be different from this version once it has been copyedited and typeset.

PLEASE CITE THIS ARTICLE AS DOI: 10.1063/1.50003590

The entire raw data used to generate the figures in the work is available at the supplement.

Acknowledgements

The authors are grateful for the support of the Israeli Science Foundation (ISF Grant 375/17). Partial support in the fabrication and characterization of the samples was provided by the Technion's Micro-Nano Fabrication Unit (MNFU) and the Russell Berrie Nanotechnology Institute (RBNI). Valentina Korchnoy and Arkadi Gavrilov are acknowledged for valuable technical assistance.

Data Availability

The data that supports the findings of this study are available within the article and its supplementary material.

References

- ¹ A. Ohtomo and H.Y. Hwang, *Nature* **427**, 423 (2004).
- ² S. Stemmer and S. James Allen, *Annu. Rev. Mater. Res.* **44**, 151 (2014).
- ³ D.V. Christensen, F. Trier, W. Niu, Y. Gan, Y. Zhang, T.S. Jespersen, Y. Chen, and N. Pryds, *Adv. Mater. Interfaces* **6**, 1900772 (2019).
- ⁴ Y.-Y. Pai, A. Tylan-Tyler, P. Irvin, and J. Levy, *Reports Prog. Phys.* **81**, 36503 (2018).
- ⁵ P. Zubko, S. Gariglio, M. Gabay, P. Ghosez, and J.-M. Triscone, *Annu. Rev. Condens. Matter Phys.* **2**, 141 (2011).
- ⁶ L. Kornblum, *Adv. Mater. Interfaces* **6**, 1900480 (2019).
- ⁷ B. Förg, C. Richter, and J. Mannhart, *Appl. Phys. Lett.* **100**, 053506 (2012).
- ⁸ N.Y. Chan, M. Zhao, J. Huang, K. Au, M.H. Wong, H.M. Yao, W. Lu, Y. Chen, C.W. Ong, H.L.W. Chan, and J. Dai, *Adv. Mater.* **26**, 5962 (2014).
- ⁹ M. Hosoda, Y. Hikita, H.Y. Hwang, and C. Bell, *Appl. Phys. Lett.* **103**, 103507 (2013).

This is the author's peer reviewed, accepted manuscript. However, the online version of record will be different from this version once it has been copyedited and typeset.

PLEASE CITE THIS ARTICLE AS DOI: 10.1063/1.50003590

- ¹⁰ M.A. Islam, D. Saldana-Greco, Z. Gu, F. Wang, E. Breckenfeld, Q. Lei, R. Xu, C.J. Hawley, X.X. Xi, L.W. Martin, A.M. Rappe, and J.E. Spanier, *Nano Lett.* **16**, 681 (2016).
- ¹¹ L. Cheng, X. Fan, L. Wei, J. Lu, H. Liang, J. Qi, and C. Zeng, *Phys. Rev. Appl.* **6**, 14005 (2016).
- ¹² S. Wu, X. Luo, S. Turner, H. Peng, W. Lin, J. Ding, A. David, B. Wang, G. Van Tendeloo, J. Wang, and T. Wu, *Phys. Rev. X* **3**, 41027 (2013).
- ¹³ S.M. Kim, H.J. Kim, H.J. Jung, S.H. Kim, J.-Y. Park, T.J. Seok, T.J. Park, and S.W. Lee, *ACS Appl. Mater. Interfaces* **11**, 30028 (2019).
- ¹⁴ C. Lin and A.A. Demkov, *Phys. Rev. Lett.* **113**, 157602 (2014).
- ¹⁵ C. Baeumer, C. Funck, A. Locatelli, T.O. Menteş, F. Genuzio, T. Heisig, F. Hensling, N. Raab, C.M. Schneider, S. Menzel, R. Waser, and R. Dittmann, *Nano Lett.* **19**, 54 (2019).
- ¹⁶ C. Funck, A. Marchewka, C. Bäumer, P.C. Schmidt, P. Müller, R. Dittmann, M. Martin, R. Waser, and S. Menzel, *Adv. Electron. Mater.* **4**, 1800062 (n.d.).
- ¹⁷ Z.Q. Liu, C.J. Li, W.M. Lü, X.H. Huang, Z. Huang, S.W. Zeng, X.P. Qiu, L.S. Huang, A. Annadi, J.S. Chen, J.M.D. Coey, T. Venkatesan, and Ariando, *Phys. Rev. X* **3**, 021010 (2013).
- ¹⁸ F. Gunkel, R. Waser, A.H.H. Ramadan, R.A. De Souza, S. Hoffmann-Eifert, and R. Dittmann, *Phys. Rev. B* **93**, 245431 (2016).
- ¹⁹ F. Gunkel, S. Hoffmann-Eifert, R.A. Heinen, D. V Christensen, Y.Z. Chen, N. Pryds, R. Waser, and R. Dittmann, *ACS Appl. Mater. Interfaces* **9**, 1086 (2017).
- ²⁰ M. Andrä, H. Bluhm, R. Dittmann, C.M. Schneider, R. Waser, D.N. Mueller, and F. Gunkel, *Phys. Rev. Mater.* **3**, 44604 (2019).
- ²¹ M. Andrä, C. Funck, N. Raab, M.-A. Rose, M. Vorokhta, F. Dvorčák, B. Šmíd, V. Matolín, D.N. Mueller, R. Dittmann, R. Waser, S. Menzel, and F. Gunkel, *Adv. Electron. Mater.* **6**, 1900808 (2020).
- ²² R. Waser, R. Dittmann, G. Staikov, and K. Szot, *Adv. Mater.* **21**, 2632 (2009).
- ²³ T. Heisig, C. Baeumer, U.N. Gries, M.P. Mueller, C. La Torre, M. Luebben, N. Raab, H. Du, S. Menzel, D.N. Mueller, C.-L. Jia, J. Mayer, R. Waser, I. Valov, R.A. De Souza, and R. Dittmann, *Adv. Mater.* **30**, 1800957 (2018).
- ²⁴ Y. Chen, N. Pryds, J.E. Kleibeuker, G. Koster, J. Sun, E. Stamate, B. Shen, G. Rijnders, and S. Linderoth, *Nano Lett.* **11**, 3774 (2011).
- ²⁵ S.W. Lee, Y. Liu, J. Heo, and R.G. Gordon, *Nano Lett.* **12**, 4775 (2012).
- ²⁶ T.J. Seok, Y. Liu, H.J. Jung, S. Bin Kim, D.H. Kim, S.M. Kim, J.H. Jang, D.-Y. Cho, S.W. Lee, and T.J. Park, *ACS Nano* **12**, 10403 (2018).
- ²⁷ H.J. Lee, T. Moon, C.H. An, and C.S. Hwang, *Adv. Electron. Mater.* **5**,

This is the author's peer reviewed, accepted manuscript. However, the online version of record will be different from this version once it has been copyedited and typeset.

PLEASE CITE THIS ARTICLE AS DOI: 10.1063/1.50003590

1800527 (2019).

²⁸ T. Moon, H.J. Jung, Y.J. Kim, M.H. Park, H.J. Kim, K. Do Kim, Y.H. Lee, S.D. Hyun, H.W. Park, S.W. Lee, and C.S. Hwang, *APL Mater.* **5**, 42301 (2016).

²⁹ J.H. Ngai, Y. Segal, F.J. Walker, and C.H. Ahn, *Phys. Rev. B* **83**, 45304 (2011).

³⁰ S.M. Walker, F.Y. Bruno, Z. Wang, A. de la Torre, S. Ricc , A. Tamai, T.K. Kim, M. Hoesch, M. Shi, M.S. Bahramy, P.D.C. King, and F. Baumberger, *Adv. Mater.* **27**, 3894 (2015).

³¹ Y. Chen, N. Pryds, J.E. Kleibeuker, G. Koster, J. Sun, E. Stamate, B. Shen, G. Rijnders, and S. Linderoth, *Nano Lett.* **11**, 3774 (2011).

³² S.W. Lee, Y.Q. Liu, J. Heo, and R.G. Gordon, *Nano Lett.* **12**, 4775 (2012).

³³ D. Miron, I. Krylov, M. Baskin, E. Yalon, and L. Kornblum, *J. Appl. Phys.* **126**, 185301 (2019).

³⁴ D. Cohen-Azarzar, M. Baskin, and L. Kornblum, *J. Appl. Phys.* **123**, 245307 (2018).

³⁵ M. Lanza, H.-S.P. Wong, E. Pop, D. Ielmini, D. Strukov, B.C. Regan, L. Larcher, M.A. Villena, J.J. Yang, L. Goux, A. Belmonte, Y. Yang, F.M. Puglisi, J. Kang, B. Magyari-K pe, E. Yalon, A. Kenyon, M. Buckwell, A. Mehonic, A. Shluger, H. Li, T.-H. Hou, B. Hudec, D. Akinwande, R. Ge, S. Ambrogio, J.B. Roldan, E. Miranda, J. Su e, K.L. Pey, X. Wu, N. Raghavan, E. Wu, W.D. Lu, G. Navarro, W. Zhang, H. Wu, R. Li, A. Holleitner, U. Wurstbauer, M.C. Lemme, M. Liu, S. Long, Q. Liu, H. Lv, A. Padovani, P. Pavan, I. Valov, X. Jing, T. Han, K. Zhu, S. Chen, F. Hui, and Y. Shi, *Adv. Electron. Mater.* **5**, 1800143 (2019).

³⁶ A. Sawa, *Mater. Today* **11**, 28 (2008).

³⁷ J. Jang, H.-H. Choi, S.H. Paik, J.K. Kim, S. Chung, and J.H. Park, *Adv. Electron. Mater.* **4**, 1800355 (2018).

³⁸ C.-Y. Lin, C.-Y. Wu, C.-Y. Wu, C. Hu, and T.-Y. Tseng, *J. Electrochem. Soc.* **154**, G189 (2007).

³⁹ *Nat. Nanotechnol.* **3**, 429 (2008).

⁴⁰ N. Pryds and V. Esposito, *J. Electroceramics* **38**, 1 (2016).

⁴¹ J. Lee, W. Schell, X. Zhu, E. Kioupakis, and W.D. Lu, *ACS Appl. Mater. Interfaces* **11**, 11579 (2019).

⁴² S. Kim, S. Choi, and W. Lu, *ACS Nano* **8**, 2369 (2014).

⁴³ X. Huang, Y. Li, H. Li, K. Xue, X. Wang, and X. Miao, *IEEE Electron Device Lett.* **41**, 549 (2020).

⁴⁴ M.J. Rozenberg, I.H. Inoue, and M.J. S nchez, *Phys. Rev. Lett.* **92**, 178302 (2004).

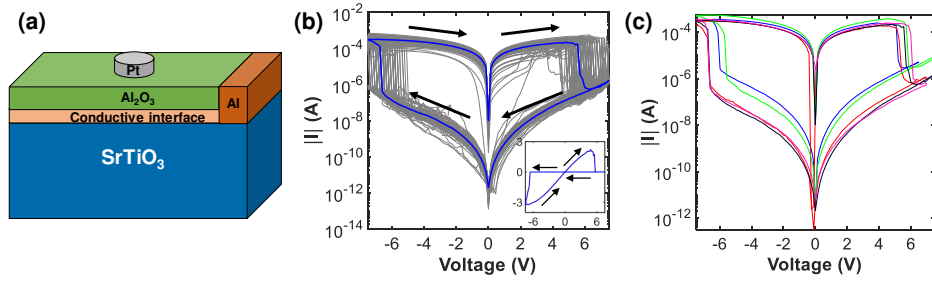
This is the author's peer reviewed, accepted manuscript. However, the online version of record will be different from this version once it has been copyedited and typeset.

PLEASE CITE THIS ARTICLE AS DOI: 10.1063/1.50003590

- ⁴⁵ C. Jooss, L. Wu, T. Beetz, R.F. Klie, M. Beleggia, M.A. Schofield, S. Schramm, J. Hoffmann, and Y. Zhu, *Proc. Natl. Acad. Sci.* **104**, 13597 LP (2007).
- ⁴⁶ S. Tsui, Y.Q. Wang, Y.Y. Xue, and C.W. Chu, *Appl. Phys. Lett.* **89**, 123502 (2006).
- ⁴⁷ M. Hamaguchi, K. Aoyama, S. Asanuma, Y. Uesu, and T. Katsufuji, *Appl. Phys. Lett.* **88**, 142508 (2006).
- ⁴⁸ A. Baikalov, Y.Q. Wang, B. Shen, B. Lorenz, S. Tsui, Y.Y. Sun, Y.Y. Xue, and C.W. Chu, *Appl. Phys. Lett.* **83**, 957 (2003).
- ⁴⁹ Y.B. Nian, J. Strozier, N.J. Wu, X. Chen, and A. Ignatiev, *Phys. Rev. Lett.* **98**, 146403 (2007).
- ⁵⁰ M. Janousch, G.I. Meijer, U. Staub, B. Delley, S.F. Karg, and B.P. Andreasson, *Adv. Mater.* **19**, 2232 (2007).
- ⁵¹ M. Quintero, P. Levy, A.G. Leyva, and M.J. Rozenberg, *Phys. Rev. Lett.* **98**, 116601 (2007).
- ⁵² A. Sawa, T. Fujii, M. Kawasaki, and Y. Tokura, *Appl. Phys. Lett.* **85**, 4073 (2004).
- ⁵³ T. Fujii, M. Kawasaki, A. Sawa, H. Akoh, Y. Kawazoe, and Y. Tokura, *Appl. Phys. Lett.* **86**, 12107 (2005).
- ⁵⁴ D. Liu, S.J. Clark, and J. Robertson, *Appl. Phys. Lett.* **96**, 32905 (2010).
- ⁵⁵ Z. Guo, F. Ambrosio, and A. Pasquarello, *Appl. Phys. Lett.* **109**, 62903 (2016).
- ⁵⁶ O.A. Dicks, J. Cottom, A.L. Shluger, and V. V Afanas'ev, *Nanotechnology* **30**, 205201 (2019).
- ⁵⁷ T. Nagata, M. Haemori, Y. Yamashita, H. Yoshikawa, Y. Iwashita, K. Kobayashi, and T. Chikyow, *Appl. Phys. Lett.* **97**, 82902 (2010).
- ⁵⁸ L. Kornblum, J.A. Rothschild, Y. Kauffmann, R. Brener, and M. Eizenberg, *Phys. Rev. B* **84**, 155317 (2011).
- ⁵⁹ Y.H. Kang, J.-H. Choi, T. Il Lee, W. Lee, and J.-M. Myoung, *Solid State Commun.* **151**, 1739 (2011).

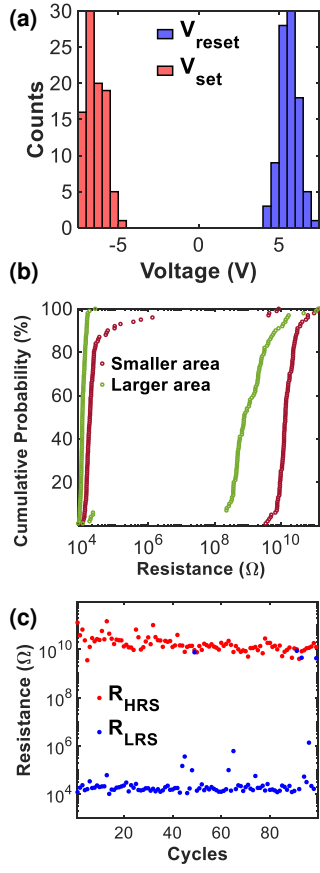
This is the author's peer reviewed, accepted manuscript. However, the online version of record will be different from this version once it has been copyedited and typeset.

PLEASE CITE THIS ARTICLE AS DOI: 10.1063/1.50003590



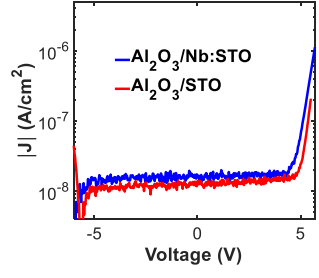
This is the author's peer reviewed, accepted manuscript. However, the online version of record will be different from this version once it has been copyedited and typeset.

PLEASE CITE THIS ARTICLE AS DOI: 10.1063/1.50003590



This is the author's peer reviewed, accepted manuscript. However, the online version of record will be different from this version once it has been copyedited and typeset.

PLEASE CITE THIS ARTICLE AS DOI: 10.1063/5.0003590



This is the author's peer reviewed, accepted manuscript. However, the online version of record will be different from this version once it has been copyedited and typeset.

PLEASE CITE THIS ARTICLE AS DOI: 10.1063/1.50003590

